Energy 93 (2015) 2102–2115

Contents lists available at ScienceDirect

Energy

journal homepage: www.elsevier.com/locate/energy

Effective reduction of NOx emissions of a HCCI (Homogeneous charge compression ignition) engine by enhanced rate of heat transfer under varying conditions of operation

T. Karthikeya Sharma*, G. Amba Prasad Rao, K. Madhu Murthy

Department of Mechanical Engineering, NIT, Warangal, 506004, T.S, India

ARTICLE INFO

Article history:
Received 18 March 2015
Received in revised form
4 October 2015
Accepted 21 October 2015
Available online 19 November 2015

Keywords:
HCCI (Homogeneous charge compression ignition) engine
ECFM-3Z Extended Coherent Flame Model-3 Zones
Rate of heat transfer
Swirl ratio
EGR (Exhaust gas recirculation)
NOx emissions

ABSTRACT

Periodic revisions in the emission norms demands refinement of engine design as well as combustion process. Of late HCCI (Homogeneous charge compression ignition) has gained interest among the combustion community for its adoption in automotive engines. Control of NOx emissions is rather difficult compared to other emissions as it interferes with in–cylinder phenomena which in turn reflect on the performance of the engine. In the present work, an attempt is made in achieving further reduction in NOx emission in HCCI mode of operation. For this purpose, premixed charge is inducted into the HCCI combustion chamber assisted with a swirl motion to enhance the convective heat transfer inside the combustion chamber. The effect of swirl in enhancing the convective heat transfer and reduction of NOx emissions was discussed in this paper. An extensive numerical experiment are conducted considering a 1.6 L single cylinder engine with a reentrant piston bowl running in HCCI mode employing a validated ECFM-3Z (Extended Coherent Flame Model-3 Zones) (STAR-CD) combustion model. Emphasis was laid on effective reduction of NOx emissions with enhanced heat transfer by simultaneously varying Boost pressure, Compression ratio, EGR (Exhaust gas recirculation) under different swirl ratios. The study revealed that higher swirl ratios play vital role in improving the convective heat transfer rate and reduction of NOx emissions. Also, it was observed that higher boost pressures & higher swirl ratios, lower EGR proportions & higher swirl ratios and higher compression ratios and higher swirl ratios are favorable in increasing the convective heat transfer. Higher compression ratios, higher boost pressures, higher EGR concentrations were observed to be favorable to reduce the NOx emissions. The results showed that apart from adopting higher compression ratios and boost pressures use of high swirl ratios is observed to be contributing to a large extent in enhancing the rates of heat transfer which would lead to significant reduction in in–cylinder temperatures suitable for low NOx emission formation in HCCI mode.

© 2015 Elsevier Ltd. All rights reserved.

1. Introduction

Internal Combustion engines have been playing a major role in the development of humankind for the last one and half century. Along with the advantages, there are many challenges associated with the engines in terms of fuel price and increased air pollution. This led the researchers to work on more efficient combustion technologies which could deliver high fuel economy and lower emissions.

The HCCI combustion concept is one such technology which delivers lowest emissions and the highest fuel economy. The lean and homogeneous mixture undergoing combustion in the combustion chamber is responsible for the advantageous associated with the HCCI engine concept. The volumetric nature of the combustion in HCCI leads to low combustion temperature and lower emissions. Along with the advantages, there are some challenges associated with the HCCI mode of combustion, which need to be addressed [1,2].

Higher combustion temperatures and engine cylinder walls facilitates the oxidation reaction between N_2 and O_2 in the combustion chamber and leads to harmful NOx emissions. Increased turbulence inside the combustion chamber increases the homogeneity of the charge and further increase in turbulence leads to

* Corresponding author.
E-mail address: karthikeya.sharma3@gmail.com (T. Karthikeya Sharma).

http://dx.doi.org/10.1016/j.energy.2015.10.083
0360-5442/© 2015 Elsevier Ltd. All rights reserved.

Nomenclature

a	crank radius
B	Cylinder bore
CFD	Computational Fluid Dynamics
CI	Compression Ignition
C_p	Specific Heat
ECFM-3Z	Extended Coherent Flame Model-3 Zones
EDDI	Experimental Direct Diesel Injection
EDVI	Experimental Diesel Vapor Induction
EGR	Exhaust Gas Recirculation
ε	dissipation rate
HCCI	Homogeneous Charge Compression Ignition
I	Turbulence Intensity
IC	Internal Combustion
ISFC	Indicated Specific Fuel Consumption
k	Turbulent Kinetic Energy
L	Length scale
l	Connecting rod length
N	Number of cylinders
n_R	Number of crank revolutions
P	Indicated power per cylinder
SDDI	Simulated Direct Diesel Injection
SDVI	Simulated Diesel Vapor Induction
SI	Spark Ignition
μ_t	Turbulent viscosity
V_∞	Velocity Magnitude

increased heat transfer from the combustion chamber. The swirl motion of the charge inside the combustion chamber leads to increased convective heat transfer from the engine. Also, swirl helps in the homogeneous mixture formation of the fuel and air [3], and helps in NOx emission reduction [4]. The increase in the swirl ratio reduces the peak temperatures by increasing the heat transfer to the combustion chamber parts. This leads to a low temperature combustion process resulting in lower NOx emissions [5]. The rate of heat transfer effecting NOx emissions was discussed in the author's previous work [6].

Dealing with so many parameters that involve complex chemical reactions and to get precise results solely in the laboratory would be inefficient, expensive, and impractical since there are many variables that exhibit complex interaction. Because of this reason, a CFD (Computational fluid dynamics) tool STAR-CD is chosen for the analysis. Several modifications were made to STAR-CD es-ice module so that it could be used for HCCI engine modeling. The different combustion models which are well developed for predicting engine processes are Transient Interactive Flamelets (TIF) model, Digital Analysis of Reaction System −Transient Interactive Flamelets model (DARS-TIF), G −equation model [7], Extended Coherent Flame Combustion Model-3 Zones [8] and the, Equilibrium-Limited ECFM (ECFM-CLEH) [9,10]. Each model has its own limitations and is suitable for a specific set of problems. Generally speaking; ECFM-3Z and ECFM-CLEH can be used for all types of combustion regime, whereas ECFM-3Z is mostly suitable for homogeneous turbulent premixed combustion with spark ignition and Compression Ignition. Various combustion models applicability's are shown in Table 1. Owing to its wide applicability, in the present work ECFM-3Z has been used to study the effect of swirl motion of intake charge on emissions and performance of HCCI engine. Fig. 1 depicts the schematic representation of the three zones of the ECFM-3Z model. This model is capable of simulating the complex mechanisms like turbulent mixing, flame propagation, diffusion combustion and pollutant emission that characterize modern IC (Internal combustion) engines.

Table 1
Combustion models capabilities.

Model	Applicability
G-Equation	Partially Premixed S.I & C.I
DARS-TIF	Compression Ignition
ECFM	Non-Homogeneous Premixed S.I.
ECFM-3Z	Premixed and Non Premixed S.I and C.I

Induction induced swirl has a predominant effect on mixture formation and rapid spreading of the flame front in the conventional combustion process of a CI engine. This has been well documented in the literature. However, it is observed that no work has been done on the effect of swirl in HCCI mode.

In the present study the effect of induction induced swirl under various parameters in enhancing the heat transfer from the HCCI engine and in reducing the NOx emissions were analyzed. Convective heat transfer was expected to increase with increase in swirl ratio and other parameters like EGR (Exhaust gas recirculation), compression ratio and boost pressure also expected to contribute in the heat transfer enhancement and reduction of NOx emissions. The increased heat transfer leading to low temperature combustion leads to reduced NOx emissions. The swirl ratio varied from 1 to 4, compression ratio was varied from 18 to 21, boost pressure was considered between 1 bar and 2 bar and EGR proportions were varied from 0% to 30%. The study of the combined effect of swirl and other parameters on Heat transfer and emissions reduction was the main objective of the present paper.

2. Methodology

A single cylinder direct injection, reentrant piston bowl, CI engine with the specifications given in Table 2 has been considered for the analysis. A CFD package STAR-CD is used with necessary modifications for the analysis to study the rates of heat transfer inside the combustion chamber with swirl and other operating parameters in CI engine HCCI Mode. The engine specifications considered for the analysis are shown in Table 2.

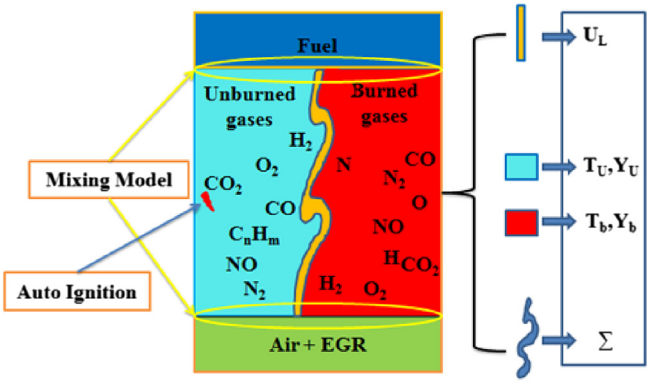

Fig. 1. Schematic representation of three zones of ECFM-3Z model.

Table 2
Engine specifications.

Engine specifications	
Displacement Volume	1600 cm^3
Bore	12.065 cm
Stroke	14 cm
Connecting rod length	26 cm
Compression ratio	21:1
Fuel	n-Dodecane
Operating conditions	
Engine speed	1000 rpm
Equivalence ratio	0.26
Inlet temperature air (T_{air})	353 K
Inlet air Pressure (P_{air})	0.1 MPa
Cylinder Wall Temperature (T_{wall})	450 K
EGR	0%

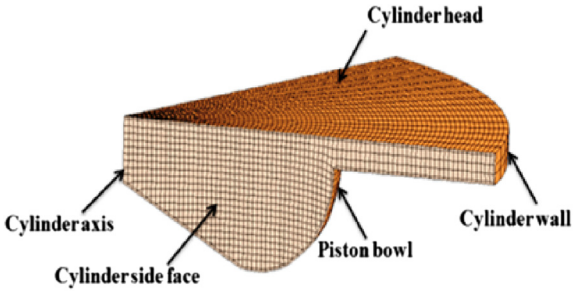

Fig. 2. Schematic representation of 3D piston bowl shape at TDC.

3. CFD model set-up

The computational mesh consists of 128,000 cells representing 1/6th of the piston bowl created in STAR-CD by generating a spline based on the piston bowl shape. A 2D template was cut by the spline to cut the 3D mesh with 40 radial cells, 160 axial cells, 5 top dead center layers and 40 axial block cells. The piston bowl shape and 3D mesh of the piston bowl sector is shown in Fig. 2.

The energy efficiency of the engine is analyzed by gross indicated work per cycle (W) calculated from the cylinder pressure and the piston displacement using Eq. (1):

$$W(Nm) = \frac{\pi a B_2}{8} \int_{\theta_1}^{\theta_2} p(\theta) \left[2\sin(\theta) \frac{a\sin(2\theta)}{\sqrt{l^2 - a^2\sin^2(\theta)}} \right] d\theta \quad (1)$$

where a, l, and B are the crank radius, connecting rod length and cylinder bore, respectively, and θ_1 and θ_2 are the beginning and the end of the valve-closing period.

The indicated power per cylinder (P) is related to the indicated work per cycle by using Eq. (2):

$$P(kW) = \frac{WN}{60000 n_R} \quad (2)$$

where $n_R = 2$ is the number of crank revolutions for each power stroke per cylinder and N is the engine speed (rpm). The indicated specific fuel consumption (ISFC) is shown in Eq. (3):

$$ISFC(g/kWh) = \frac{30 m_{fuel} N}{P} \quad (3)$$

In Eq. (1), the power and ISFC analyses can be viewed as being only qualitative rather than quantitative in this study.

4. Modeling strategy

The STAR-CD used in the present study has integrated several sub models such as turbulence, fuel spray and atomization, wall function, ignition, combustion, NOx, and soot models for various types of combustion modes in CI as well as SI engine computations. As initial values of k and ε are not known a priori the turbulence initialization is done using I-L model. For this purpose local turbulence intensity I, and length scale L, is related as

$$k_\infty = (3/2) I^2 V_\infty^2 \quad (4)$$

$$\varepsilon_\infty = C_\mu^{3/4} \left(k_\infty^{3/2} / L \right) \quad (5)$$

This practice will ensure that k and ε and the turbulent viscosity μ_t, will all scale correctly with V_∞, which is desirable from both the physical realism and numerical stability point of view. Moreover the turbulent intensity is defined using the same velocity vector magnitude as that of stagnation quantities.

The combustion is modeled using ECFM-3Z. As far as fluid properties are concerned, ideal gas law and temperature dependent constant pressure specific heat (C_p) are chosen.

The ECFM-3Z incorporates the following models in its operation.

Phenomena	Model
▪ Spray injection and Atomization	Huh (1991)
▪ Auto Ignition model	Double delay auto ignition
▪ Combustion	ECFM-3Z Compression Ignition (Colin and Benkenida, 2004)
▪ Turbulence	Intensity–Length scale
▪ Droplet breakup	Reitz–Diwakar (1986)
▪ Liquid Film	Angelberger et al. (1997)
▪ Droplet wall interaction	Bai and Gosman (1996)
▪ Boiling	Rohsenow (1952)
▪ NOx mechanism	Extended Zel'dovich mechanism
▪ Soot	Mauss and Karlson (2006)

5. Initial and boundary conditions

To begin with, an absolute pressure 1.02 bar, with 0% EGR, temperature to 353 K, equivalence ratio as 0.26 are taken as initial values. Fixed boundary wall temperatures are taken with combustion dome regions as 450 K, piston crown regions as 450 K, and cylinder wall regions as 400 K. The Angleberger wall function mode is considered [11]. The 'two-layer' and low Reynolds number approaches, where no-slip conditions are applied directly and the boundary layers are computed by solving the mass, momentum and turbulence equations (the latter in their 'low Reynolds number' form) within them. The hybrid wall boundary condition which is a

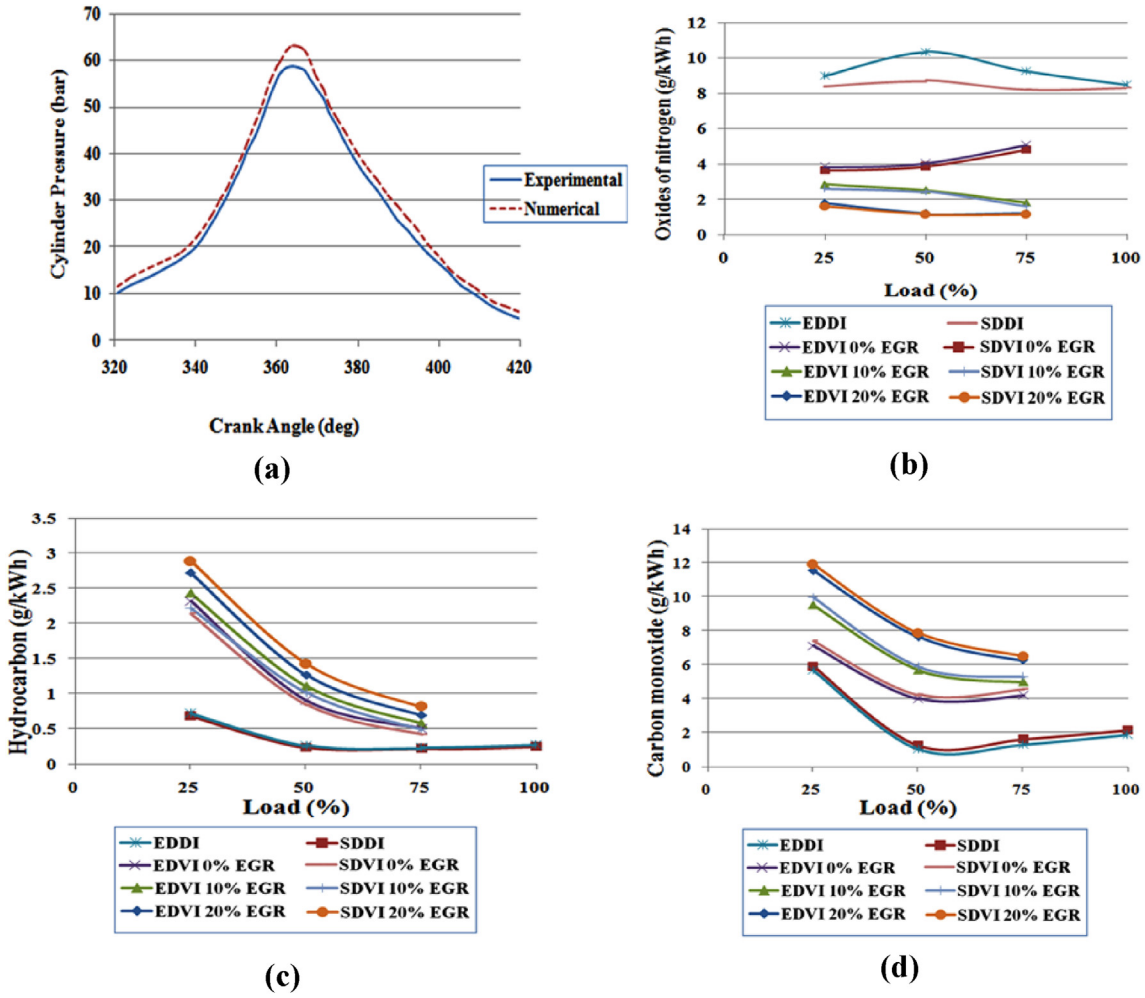

Fig. 3. Validation of the ECFM-3Z Compression Ignition Model with the experimental results of External mixture formation of HCCI engine.

combination of two layered and low-Reynolds number wall boundary conditions are considered in this analysis. This hybrid wall boundary condition removes the burden of having to ensure a small enough near-wall value for y^+ (by creating a sufficiently fine mesh next to the wall). The y^+ independency of the hybrid wall condition is achieved using either an asymptotic expression valid for $0.1 < y^+ < 100$ or by blending low-Reynolds and high-Reynolds number expressions for shear stress, thermal energy and chemical species wall fluxes. This treatment provides valid boundary conditions for momentum, turbulence, energy and species variables for a wide range of near-wall mesh densities.

Standard wall functions are used to calculate the variables at the near wall cells and the corresponding quantities on the wall. The initial conditions were specified at IVC, consisting of a quiescent flow field at pressure and temperature for full load condition.

6. Validation of ECFM-3Z

STAR-CD is a well known Commercial CFD package being adopted many renowned researchers and well established research organizations in the field of automotive IC engines. The results obtained through this package are validated with the experimental results by many authors like Pasupathy Venkateswaran [4] et al., Zellat Marc [12] et al., Bakhshan [13] et al. A comparison of the CI engine in HCCI is done in this paper considering the extended coherent flame combustion three zones, a compression model for combustion analysis. The present paper deals with the simulation of CI engine in HCCI mode, using a fuel vaporizer to achieve excellent HCCI combustion in a single cylinder air-cooled direct injection diesel engine. No modifications were made to the combustion system. Ganesh and Nagarajan [14] conducted experiments with diesel vapor induction without EGR and diesel vapor induction with 0%, 10% and 20% EGR. Validation of the present model with the experimental results of Ganesh and Nagarajan [14] was done by considering all the engine specifications.

Ganesh and Nagarajan [14] considered a vaporized diesel fuel with air to form a homogeneous mixture and inducted into the cylinder during the intake stroke. To control the early ignition of diesel vapor–air mixture, cooled (30 °C) Exhaust Gas Recirculation (EGR) technique was adopted. For the validation purpose, the results are compared with respect to engine performance and emissions in the following figures. It is observed that the simulated results are in good agreement with the experimental results. The comparison of the plots between simulation and experimental results is shown in Fig. 3. In the figures EDVI (Experimental diesel vapor induction) represents the experimental diesel vapor injection and SDVI (simulated diesel vapor induction) represents simulated diesel vapor induction at respective EGR concentrations.

7. Results and discussion

In the present paper the effect of induced swirl and other operating parameters like compression ratio and boost pressure on the heat transfer rate is studied. The swirl ratios ranging from 1 to 4

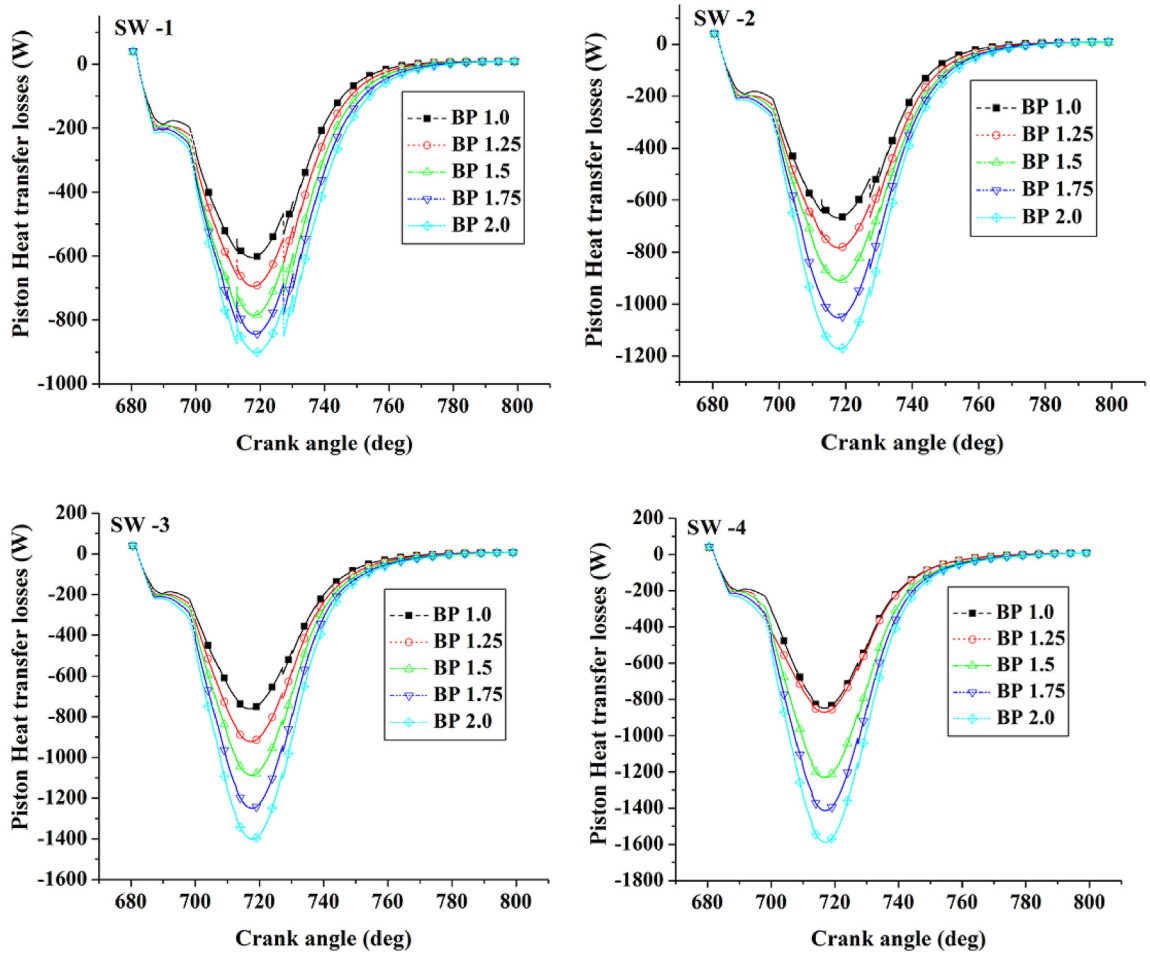

Fig. 4. Heat transfer to the piston Vs Crank angle at different boost pressures and swirl ratios.

are considered for the analysis. The simulation results of the ECFM-3Z model are discussed below.

7.1. Heat transfer to the piston Vs boost pressure (BP)

The variation of heat transfer to the piston with boost pressure for swirl ratios 1 to 4 is plotted in Fig. 4. From Table 3, it can be observed that higher boost pressures and higher swirl ratios are favorable in increasing the heat transfer to the piston. The heat transfer rates obtained at different boost pressures and swirl ratios are summarized in Table 3. The heat transfer to the piston increases with increase in boost pressure irrespective of the swirl ratio, but the percentage increase in heat transfer is high at high swirl ratios. As swirl ratio increases; increased heat transfer rates are obtained at all boost pressures, but the increase in heat transfer rates is high at higher compression ratios [15]. The reason for this phenomenon is increasing in turbulence owing to increased wall heat transfer due to the increased swirl intensity.

7.2. Heat transfer to the walls Vs boost pressure (BP)

The variation of heat transfer to the walls with boost pressure for swirl ratios 1to 4 is plotted in Fig. 5. The heat transfer rates obtained at different boost pressures and swirl ratios are summarized in Table 4. From Table 4, it can be observed that higher boost pressures and higher swirl ratios are favorable in increasing the heat transfer to the walls [16]. The heat transfer to the walls increases with increase in boost pressure irrespective of the swirl ratio, but the percentage increase in heat transfer is higher at higher swirl ratios. As swirl ratio increases; increased heat transfer rates are obtained at all boost pressures, but the increase in heat transfer rates is high at boost pressure 1.5 bar. The reason for this

Table 3
Heat Transfer to the dome (W) at various boost pressures and swirl ratios.

BP (bar) piston	SW1	SW2	SW3	SW4	Percentage increase between SW1–SW4
BP 1.0	−605.147	−668.234	−760.625	−847.185	**39.99**
BP 1.25	−695.316	−783.45	−921.533	−870.235	**25.15**
BP 1.5	−786.091	−909.186	−1086.87	−1230.32	**56.51**
BP 1.75	−843.802	−1052.96	−1249.11	−1413.43	**67.50**
BP 2.0	−900.895	−1173.55	−1401.41	−1588.69	**76.34**
Percentage increase between BP 1.0–BP 2.0	**48.87**	**75.61**	**84.24**	**87.52**	

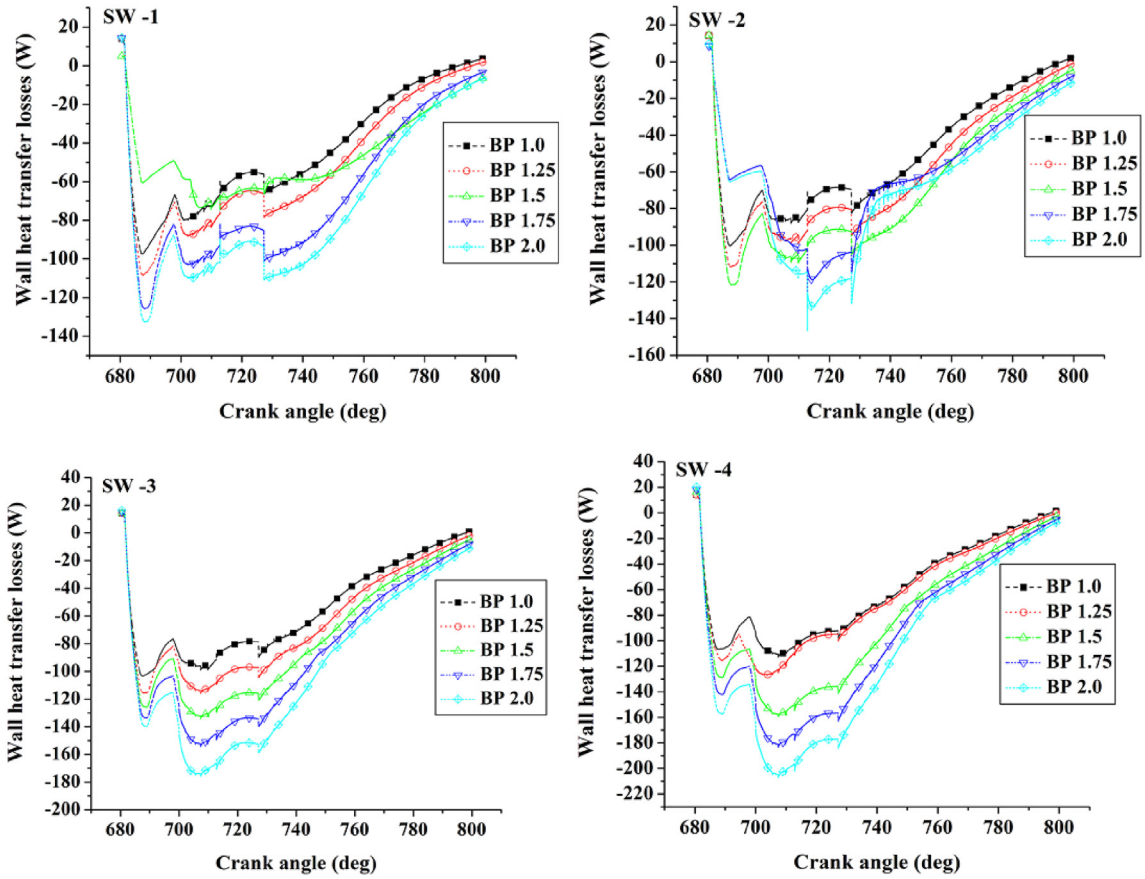

Fig. 5. Heat transfer to the walls Vs Crank angle at different boost pressures and swirl ratios.

Table 4
Heat Transfer to the walls (W) at various boost pressures and swirl ratios.

BP (bar) wall	SW1	SW2	SW3	SW4	Percentage increase between SW1–SW4
BP 1.0	−97.323	−100.373	−103.454	−112.726	**15.82**
BP 1.25	−108.397	−111.858	−115.963	−127.434	**17.56**
BP 1.5	−112.6852	−121.664	−134.296	−179.592	**59.37**
BP 1.75	−125.707	−130.442	−154.338	−183.404	**45.89**
BP 2.0	−132.643	−146.525	−175.965	−207.142	**56.16**
Percentage increase between BP 1.0–BP 2.0	**36.29**	**45.98**	**70.09**	**83.75**	

phenomenon is increasing in turbulence owing to increased wall heat transfer due to increased swirl intensity and increases in boost pressure increases the combustion chamber temperatures this increases the heat transfer at higher boost pressures when compared with lower swirl ratios.

7.3. Heat transfer to the dome Vs boost pressure (BP)

The variation of heat transfer to the dome with boost pressure for swirl ratios 1to 4 is plotted in Fig. 6. The heat transfer rates obtained at different boost pressure and swirl ratios are summarized in Table 5. From Table 5, it can be observed that higher boost pressures and higher swirl ratios are favorable in increasing the heat transfer to the dome [17]. The heat transfer to the dome increases with increase in boost pressure irrespective of the swirl ratio, but the percentage increase in heat transfer is high at swirl ratio 3. As swirl ratio increases; increased heat transfer rates are obtained at all boost pressures, but the increase in heat transfer rates is higher at higher boost pressures [18]. The reason for this

phenomenon is increasing in turbulence owing to increased wall heat transfer due to increased swirl intensity and increases in boost pressure increases the combustion chamber temperatures this increases the heat transfer at higher boost pressures when compared with lower swirl ratios.

7.4. NOx emissions

The formation of NO_X is highly dependent on the in–cylinder temperatures, oxygen concentration and residence time for the reaction to take place. From Fig. 7 it can be observed that with an increase in boost pressure the NOx emissions are getting decreased. NOx emissions are highly temperature sensitive, even below the thermal NO temperature limit. The increase in boost pressure reduces the need for preheating, facilitating the low temperature combustion resulting in lower NOx emissions. The NOx is one order of magnitude lower with two bar boost pressure than in the naturally aspirated case [19]. With the increase in swirl ratio the NOx emissions decrease irrespective of boost pressure; increased

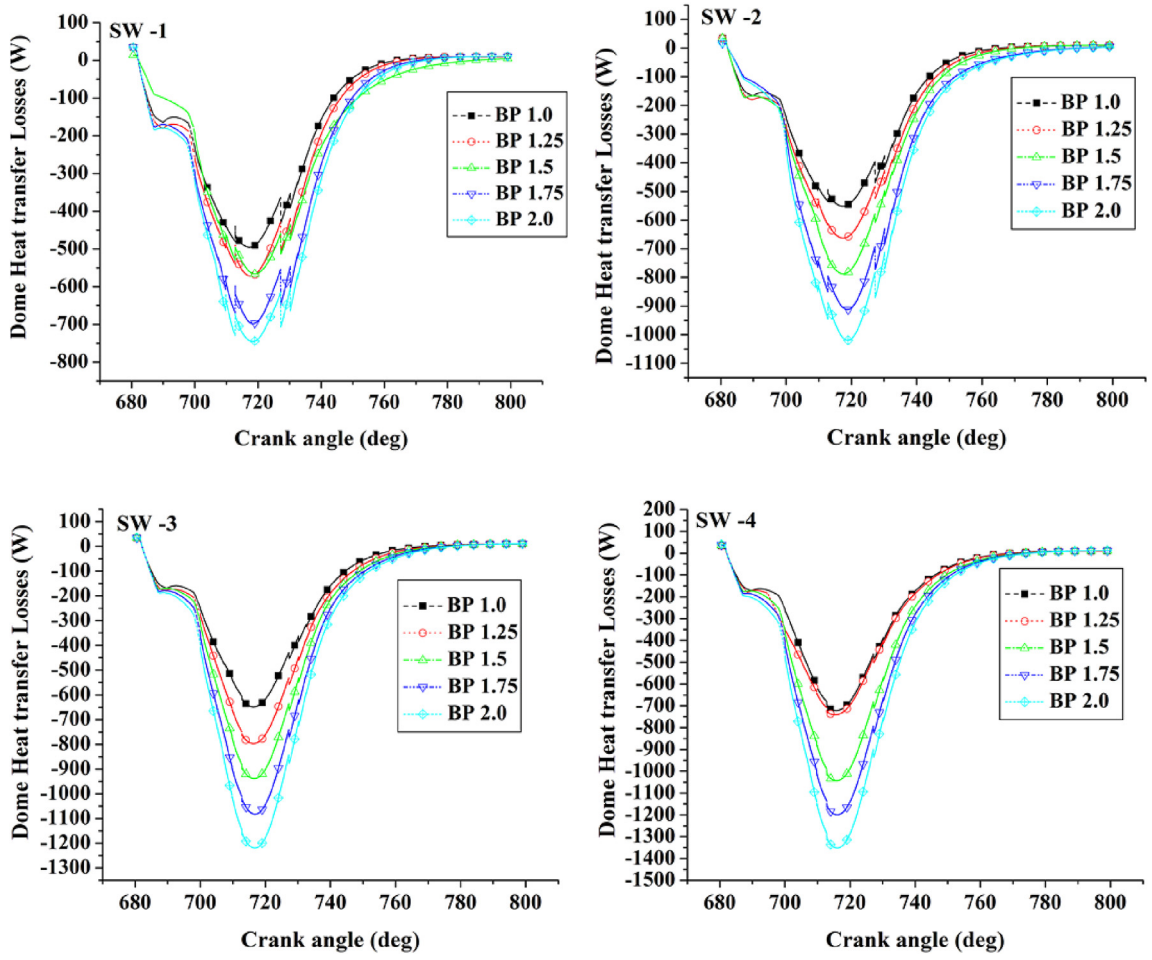

Fig. 6. Heat transfer to the dome Vs Crank angle at different boost pressures and swirl ratios.

wall heat transfer losses at higher swirl ratios causes this effect. This signifies that higher swirl ratios and higher boost pressures are favorable for low NO_x emissions.

Out of the entire range of boost pressures the lowest NOx emissions were obtained at 2 bar, proving it to be the optimum boost pressure of this particular engine. Low NOx emissions of 0.00118 g/kg fuel and 0.00133 g/kg fuel are obtained when the engine runs with 1 bar and 2 bar boost pressure at swirl ratio 4. Thus, a total decrease of 12.711% in NOx emissions was obtained when the boost pressure increased from 1 bar to 2 bar at swirl ratio 4. The NOx emissions obtained at swirl ratio 4 are low when compared to swirl ratio 1.

7.5. Heat transfer to the piston Vs EGR

The variation of heat transfer to the piston with EGR for swirl ratios 1 to 4 is plotted in Fig. 8. From Table 6, it can be observed that

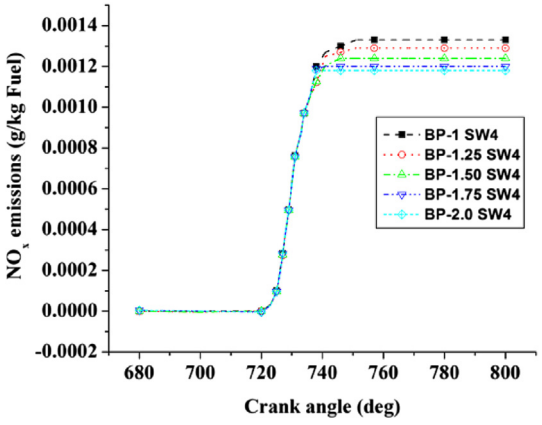

Fig. 7. NO_x emissions Vs Crank angle.

Table 5
Heat Transfer to the dome (W) at various boost pressures and swirl ratios.

BP (bar) dome	SW1	SW2	SW3	SW4	Percentage increase between SW1–SW4
BP 1.0	−495.458	−551.386	−648.456	−721.727	**45.66**
BP 1.25	−572.042	−662.761	−797.006	−740.771	**29.49**
BP 1.5	−596.358	−787.685	−938.884	−1043.16	**74.18**
BP 1.75	−698.13	−912.216	−1082.9	−1199.52	**71.81**
BP 2.0	−745.41	−1019.67	−1219.41	−1351.64	**81.32**
Percentage increase between BP 1.0–BP 2.0	**50.44**	**84.92**	**88.04**	**87.27**	

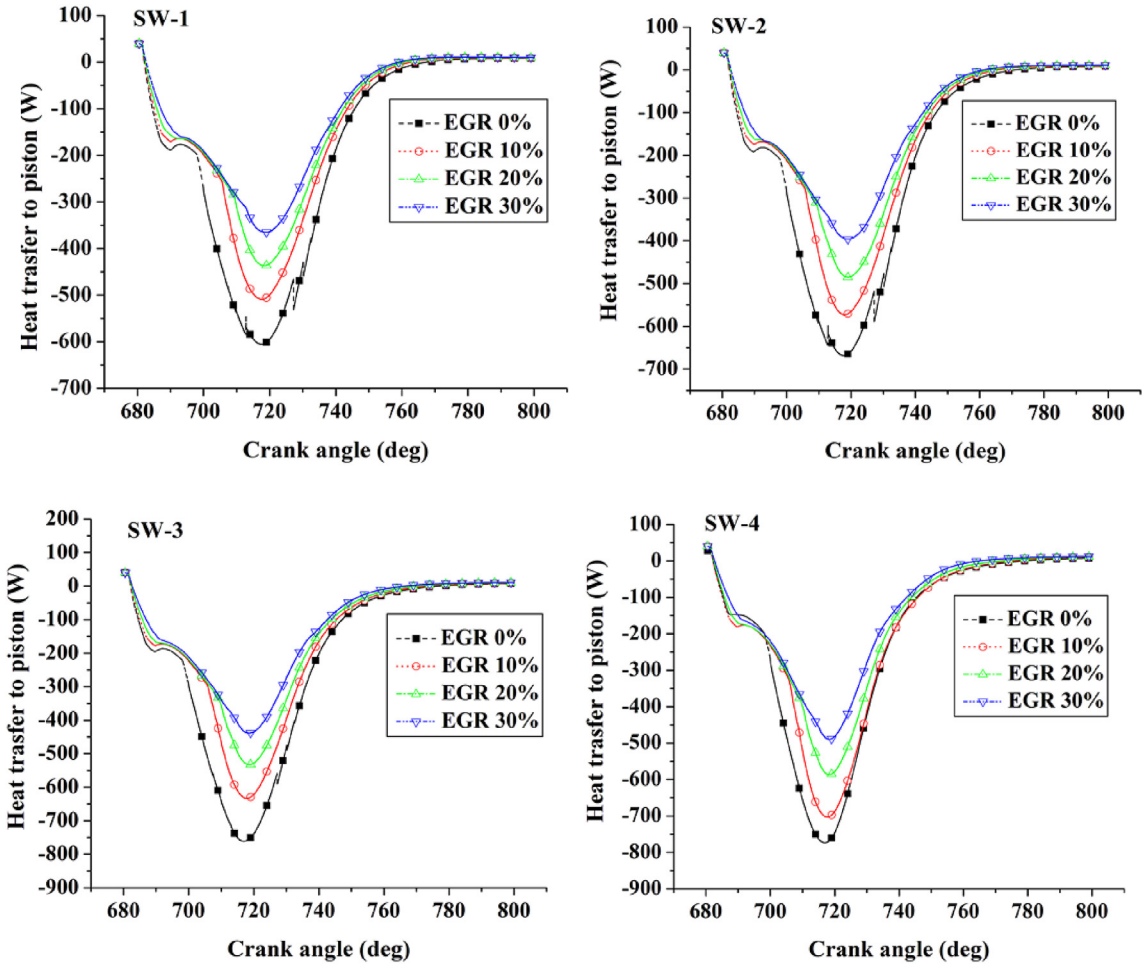

Fig. 8. Heat transfer to the piston Vs Crank angle at different EGR fractions and swirl ratios.

lower EGR proportions and higher swirl ratios are favorable in increasing the heat transfer to the piston. The heat transfer rates obtained at different EGR proportions and swirl ratios are summarized in Table 6. The heat transfer to the piston decreases with increase in EGR irrespective of the swirl ratio, but the percentage decrease in heat transfer is less at high swirl ratios and more at high swirl ratios. As swirl ratio increases; increased heat transfer rates are obtained at all EGR fractions, but the increase in heat transfer rates is higher at lower EGR fractions. The reason for this phenomenon is increasing in turbulence owing to increased wall heat transfer due to the increased swirl intensity.

7.6. Heat transfer to the walls Vs EGR

The variation of heat transfer to the walls with EGR concentration for swirl ratios 1to 4 is plotted in Fig. 9. The heat transfer rates obtained at different EGR concentrations and swirl ratios are summarized in Table 7. From Table 7, it can be observed that lower EGR concentrations and higher swirl ratios are favorable in increasing the heat transfer to the walls [20]. The rate of heat transfer to the walls decreases with increase in EGR fractions irrespective of the swirl ratio, but the percentage decrease in heat transfer is higher at lower swirl ratios and less at higher swirl ratios.

As swirl ratio increases; increased heat transfer rates are obtained at all EGR proportions, but the increase in heat transfer rates is higher at higher EGR concentrations. The reason for this phenomenon is increasing in turbulence owing to increased wall heat transfer due to the increased swirl intensity and an increase in EGR concentration helped in increasing the convective heat transfer by increasing the turbulence inside the combustion chamber.

7.7. Heat transfer to the dome Vs EGR

The variation of heat transfer to the dome with different EGR fractions for swirl ratios 1 to 4 is plotted in Fig. 10. The heat transfer rates obtained at different compression ratios and swirl ratios are

Table 6
Heat Transfer to the piston (W) at various EGR concentrations and swirl ratios.

EGR piston	SW1	SW2	SW3	SW4	Percentage increase between SW1–SW4
EGR 0%	−605.147	−668.116	−759.844	−772.635	**27.67**
EGR 10%	−508.894	−572.49	−632.831	−702.794	**38.10**
EGR 20%	−436.021	−485.007	−532.11	−584.741	**34.10**
EGR 30%	−365.313	−395.937	−437.941	−488.21	**33.64**
Percentage decrease between EGR 0%–30%	**39.63**	**40.73**	**42.36**	**36.81**	

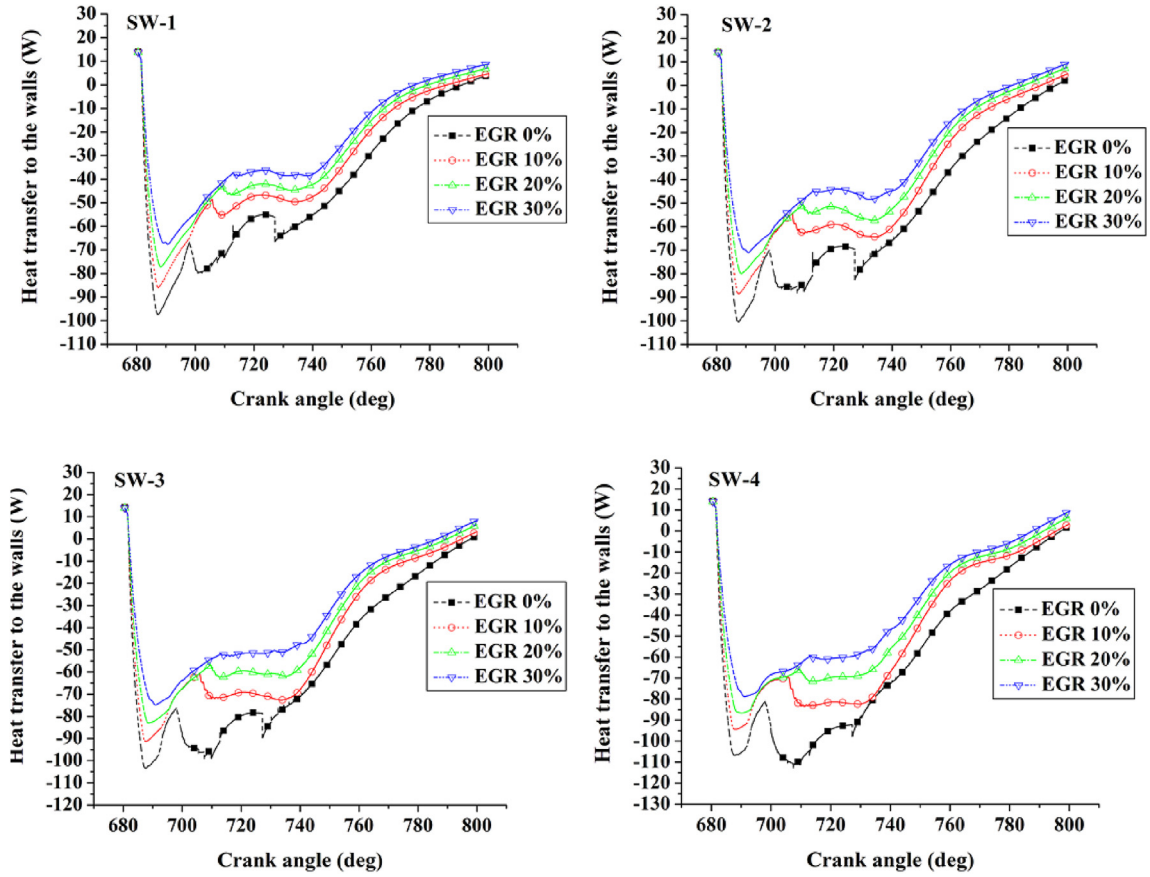

Fig. 9. Heat transfer to the walls Vs Crank angle at different EGR fractions and swirl ratios.

summarized in Table 8. From Table 8, it can be observed that lower EGR concentrations and higher swirl ratios are favorable in increasing the heat transfer to the dome. The heat transfer to the dome decreases with increase in EGR fraction irrespective of the swirl ratio, but the percentage decreases in heat transfer are low at lower swirl ratios. As swirl ratio increases; increased heat transfer rates are obtained at all EGR concentrations, but the increase in heat transfer rates is higher at lower EGR concentrations.

The reason behind it is increased swirl increased the convective heat transfer by increasing the turbulence inside the combustion chamber and the increased EGR fractions reduced the combustion temperatures leading to less temperature difference between the combustion gasses and cylinder walls.

7.8. NO_x emissions

The formation of NO_X is highly dependent on the in−cylinder temperatures, oxygen concentration and residence time for the reaction to take place. As the in−cylinder temperatures have not increased with swirl intensity, significant reduction in NO_x emissions with an increase in swirl is obtained as shown in Fig. 11. Another reason for the reduced NO_x emission could be detaining of the oxidation of the atmospheric N_2 to react with the available O_2, to form NO_x which usually occurs at high temperatures [21].

Irrespective of EGR concentration NO_x emissions reduced to increase in swirl ratio, the same trend is observed to increase in EGR concentration at all the swirl ratios. This concludes that higher swirl ratio and higher EGR concentrations favorable for low NO_x emissions. NO_x emissions of 0.00191 g/kg fuel and 0.00109 g/kg fuel are obtained with 0% and 30% EGR concentration at swirl ratio 4 was obtained. A total decrease of 42.93% in NO_x emissions was obtained when the EGR concentration was increased from 0% to 30% with swirl ratio 4.

7.9. Heat transfer to the piston Vs compression ratio

The variation of heat transfer to the piston with compression ratio for swirl ratios 1 to 4 is plotted in Fig. 12. From Table 9, it can be observed that higher compression ratios and higher swirl ratios are favorable in increasing the heat transfer to the piston. The heat

Table 7
Heat Transfer to the cylinder wall (W) at various EGR concentrations and swirl ratios.

EGR wall	SW1	SW2	SW3	SW4	Percentage increase between SW1−SW4
EGR 0%	−97.323	−100.373	−103.454	−106.676	**9.610**
EGR 10%	−86.0337	−88.5918	−91.3298	−94.2377	**9.53**
EGR 20%	−77.262	−79.7791	−82.4304	−85.245	**10.33**
EGR 30%	−67.6348	−70.9567	−74.5813	−78.3146	**15.79**
Percentage decrease between EGR 0%−30%	**30.50**	**29.30**	**27.90**	**26.58**	

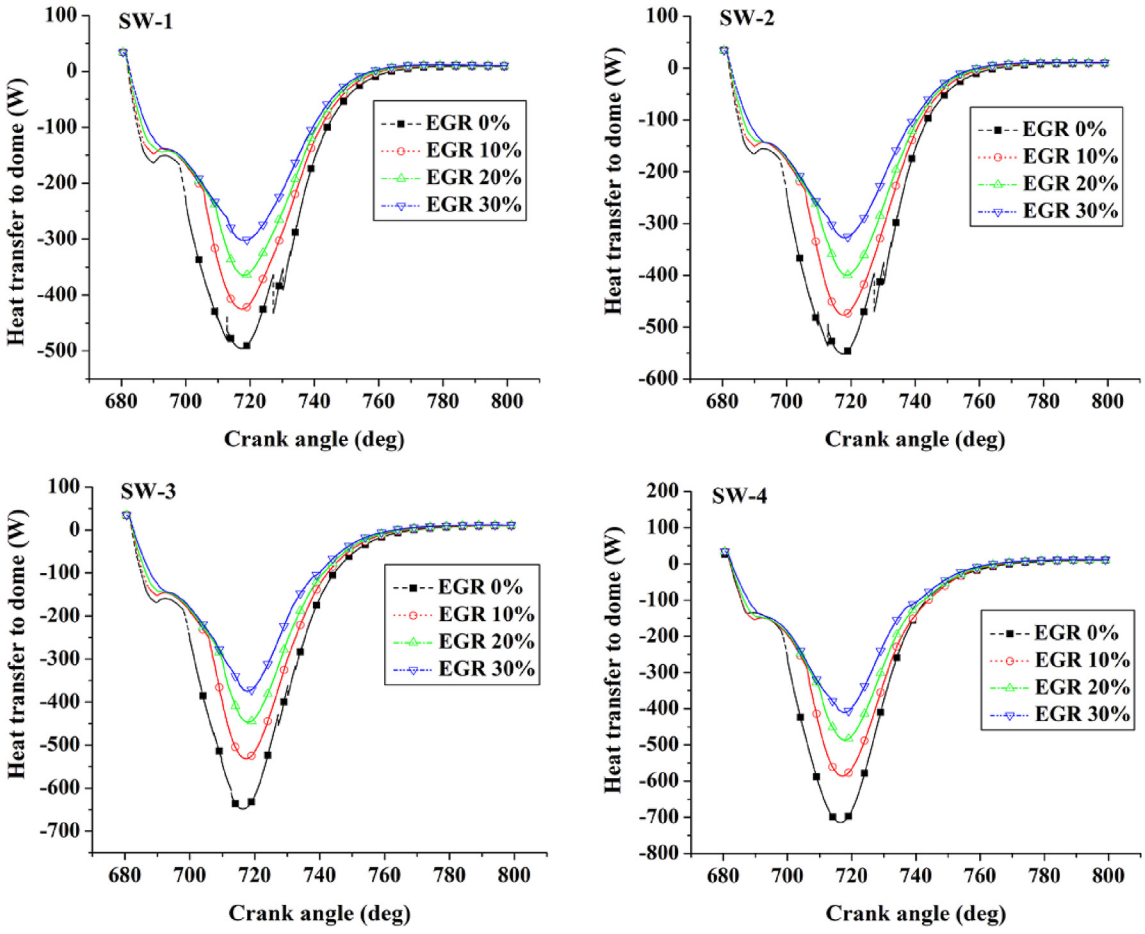

Fig. 10. Heat transfer to the domes Vs Crank angle at different EGR concentrations and swirl ratios.

Table 8
Heat Transfer to the dome (W) at various EGR fractions and swirl ratios.

EGR dome	SW1	SW2	SW3	SW4	Percentage increase between SW1–SW4
EGR 0%	−495.458	−551.37	−646.293	−712.808	**43.86**
EGR 10%	−425.46	−476.555	−531.781	−585.473	**37.60**
EGR 20%	−364.358	−399.726	−445.753	−484.729	**33.03**
EGR 30%	−302.285	−327.563	−374.425	−410.231	**35.71**
Percentage decrease between EGR 0%–30%	**38.98**	**40.59**	**42.06**	**42.44**	

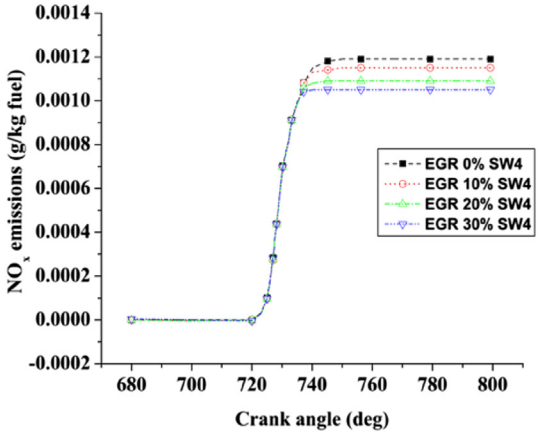

Fig. 11. NO_x emissions Vs Crank angle.

transfer rates obtained at different compression ratios and swirl ratios are summarized in Table 9.

The heat transfer to the piston increases with increase in compression ratio irrespective of the swirl ratio, but the percentage increase in heat transfer is less at low swirl ratios and more at high swirl ratios. As swirl ratio increases; increased heat transfer rates are obtained at all compression ratios, but the increase in heat transfer rates is higher at higher compression ratios. The reason for this phenomenon is increasing in turbulence owing to the increased wall heat transfer due to the increased swirl intensity.

7.10. Heat transfer to the walls Vs compression ratio

The variation of heat transfer to the walls with compression ratio of swirl ratios 1 to 4 is plotted in Fig. 13. The heat transfer rates obtained at different compression ratios and swirl ratios are summarized in Table 10. From Table 10, it can be observed that higher compression ratios and higher swirl ratios are favorable in

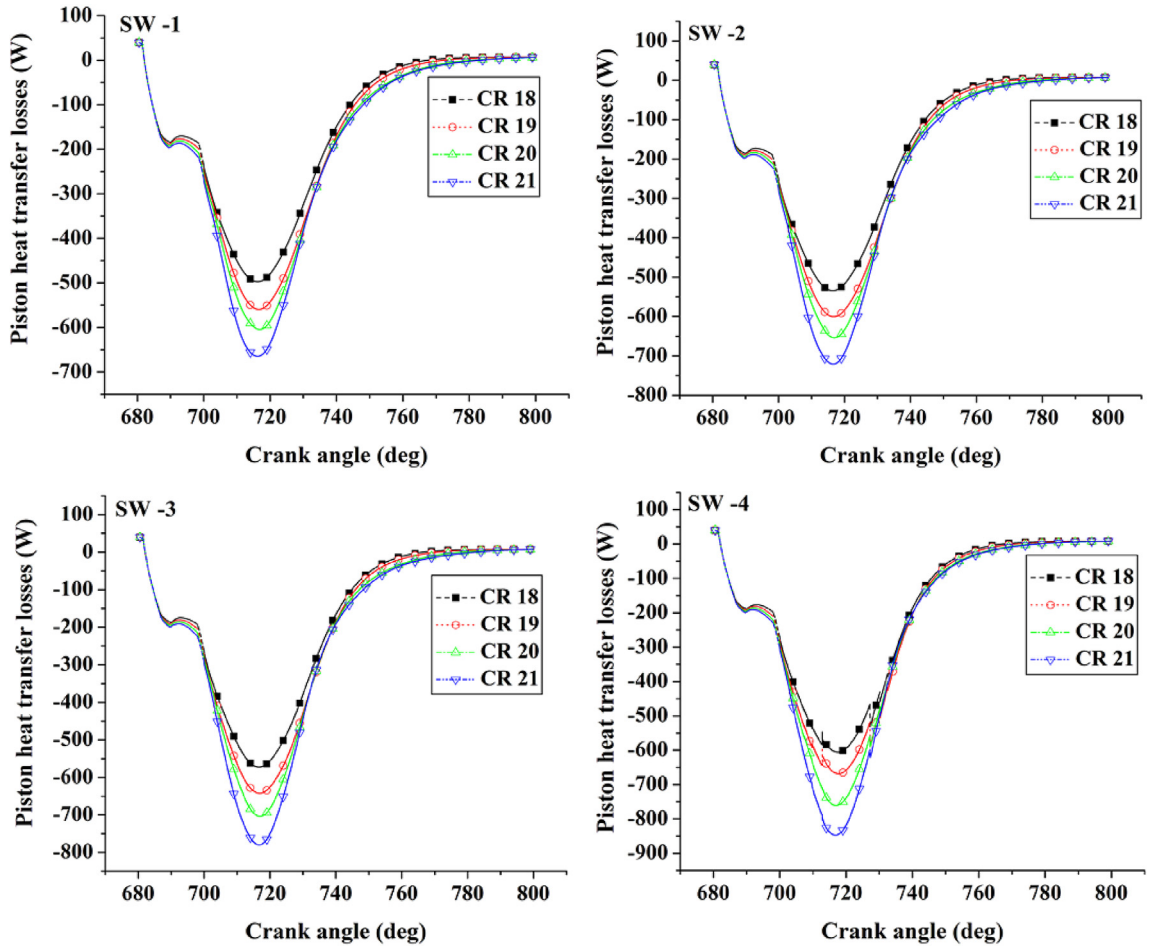

Fig. 12. Heat transfer to the piston Vs Crank angle at different compression ratios and swirl ratios.

increasing the heat transfer to the walls [22]. The rate of heat transfer to the walls decreases with increase in compression ratio irrespective of the swirl ratio, but the percentage decrease in heat transfer is higher at lower swirl ratios and less at higher swirl ratios. As swirl ratio increases; increased heat transfer rates are obtained at all compression ratios, but the increase in heat transfer rates is higher at higher compression ratios.

The reason for this phenomenon is increasing in turbulence owing to increased wall heat transfer due to the increased swirl intensity and increases in compression increases the combustion chamber temperatures this increases the heat transfer at higher compression ratios when compared with lower swirl ratios.

7.11. Heat transfer to the dome Vs compression ratio

The variation of heat transfer to the dome with compression ratio for swirl ratios 1 to 4 is plotted in Fig. 14. The heat transfer rates obtained at different compression ratios and swirl ratios are summarized in Table 11. From Table 11, it can be observed that higher compression ratios and higher swirl ratios are favorable in increasing the heat transfer to the dome [23]. The heat transfer to the dome increases with increase in compression ratio irrespective of the swirl ratio, but the percentage increase in heat transfer is higher at higher swirl ratios. As swirl ratio increases; increased heat transfer rates are obtained at all compression ratios, but the increase in heat transfer rates is higher at higher compression ratios. The reason for this phenomenon is increasing in turbulence owing to increased wall heat transfer due to the increased swirl intensity and increases in compression increases the combustion chamber temperatures this increases the heat transfer at higher compression ratios when compared with lower swirl ratios.

7.12. NO_x emissions

The formation of NO_X is highly dependent on the in−cylinder temperatures, oxygen concentration and residence time for the reaction to take place. NO_x emissions decrease with increase in swirl ratio as the in−cylinder temperatures decreases with increase

Table 9
Heat Transfer to the piston (W) at various compression ratios and swirl ratios.

Compression ratio piston	SW1	SW2	SW3	SW4	Percentage increase between SW1−SW4
CR 18	−497.279	−534.548	−572.621	−605.147	**21.69**
CR 19	−559.89	−600.553	−642.503	−668.234	**19.35**
CR 20	−604.907	−653.655	−703.826	−760.625	**25.74**
CR 21	−664.658	−720.865	−780.307	−847.185	**27.46**
Percentage Increase between CR 18-CR 21	**33.65**	**34.85**	**36.26**	**39.99**	

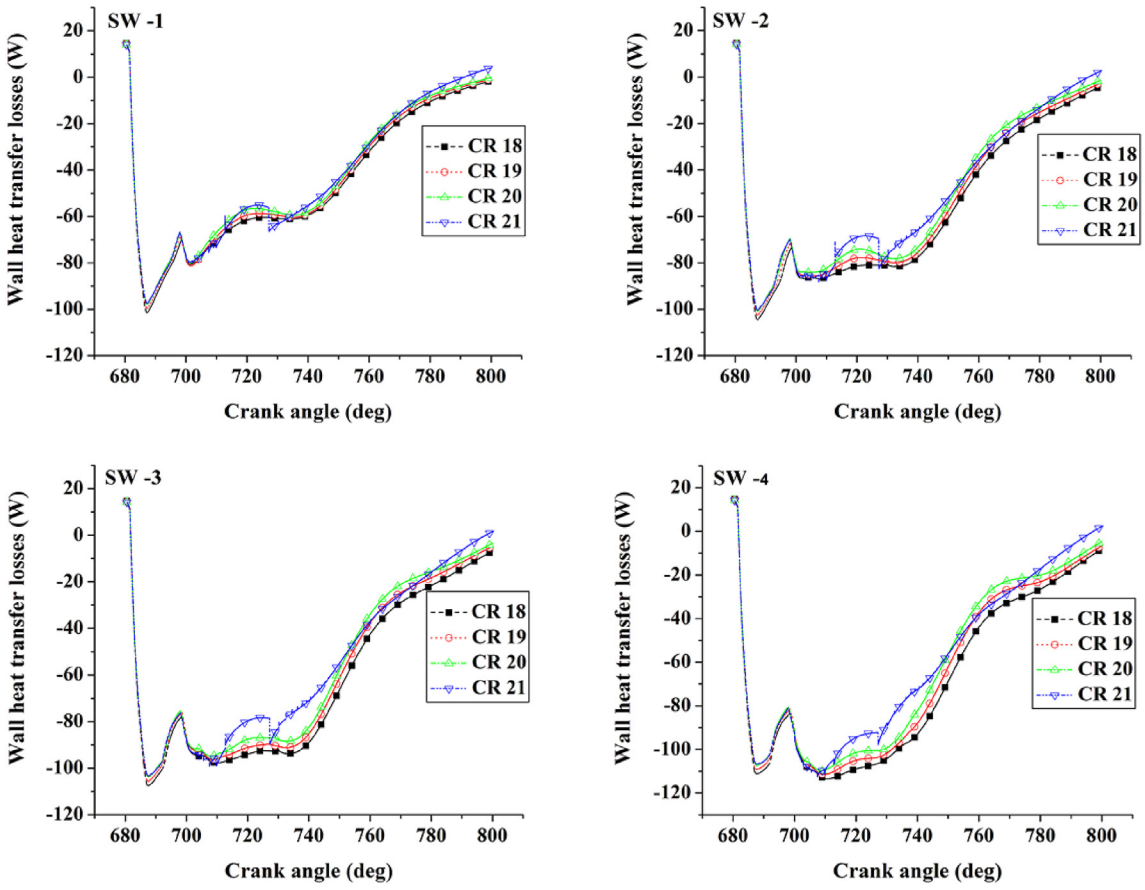

Fig. 13. Heat transfer to the walls Vs Crank angle at different compression ratios and swirl ratios.

in swirl ratios. With an increase in compression ratio NO_x emissions decreases though the in−cylinder temperatures and pressure increases [24]. The variation of NOx emissions with compression ratio and the swirl ratio can be seen from Fig. 15.

The NO_x generation also depends the time of exposure of gasses inside the combustion chamber to high temperatures, but with increase in compression ratios the exposure time reduces resulting in reduced NO_x emissions. Irrespective of CR NO_x emissions reduced with increase in swirl ratio, same trend is observed with increase in CR at all the swirl ratios. This concludes that higher swirl ratios and higher CR are favorable for low NO_x emissions. NO_x emissions of 0.001091 g/kg fuel and 0.00123 g/kg fuel are obtained with 18 and 21 CR c at swirl ratio 4 was obtained. A total decrease of 11.300% in NO_x emissions was obtained when the CR was increased from 18 to 21 at swirl ratio 4.

8. Conclusions

In the present analysis HCCI mode of combustion using premixed charge was successfully simulated using ECFM-3Z under induction induced swirl and different parameters like boost pressure, EGR and compression ratio. Analysis was done to study the effect of these parameters in enhancing the convective heat transfer in the combustion chamber to reduce the NOx emissions.

The results of the analysis showed that the enhancement of convective heat transfer and reduction of NOx emissions can be achieved by employing induction induced swirl precisely in addition to other parameters. From the results it was observed that a maximum increased heat transfer rates of 83.75% to the wall with swirl ratio 4, 88.04% to the dome with swirl ratio 3 and 87.52% to the piston with swirl ratio 4; when the boost pressures are increased from 1 bar to 2 bar were achieved. A maximum increase in heat transfer rates of 59.35% to the wall with boost pressure 1.5 bar, 81.32% to the dome and 76.34% to the piston with boost pressure 2 bar; when the swirl ratio is increased from 1 to 4 were obtained.

The NOx emission reduction was observed with increase in swirl ratio, with higher compression ratio, higher EGR and higher boost pressures. With increase in EGR concentration the convective heat transfer was observed to be reducing. A decrease of 36.81% to piston, 26.58% to wall and 38.98% to dome in heat transfer rate was decreased when the swirl ratio was increased from 1 to 4. With

Table 10
Heat Transfer to the piston (W) at various compression ratios and swirl ratios.

Wall	SW1	SW2	SW3	SW4	Percentage increase between SW1−SW4
CR 18	−101.424	−104.492	−107.676	−113.738	**12.14**
CR 19	−99.4872	−102.53	−105.736	−111.741	**12.31**
CR 20	−97.7564	−100.806	−103.903	−109.828	**12.34**
CR 21	−97.323	−100.373	−103.454	−112.726	**15.82**
Percentage reduction between CR 18-CR 21	**4.04**	**3.94**	**3.92**	**0.88**	

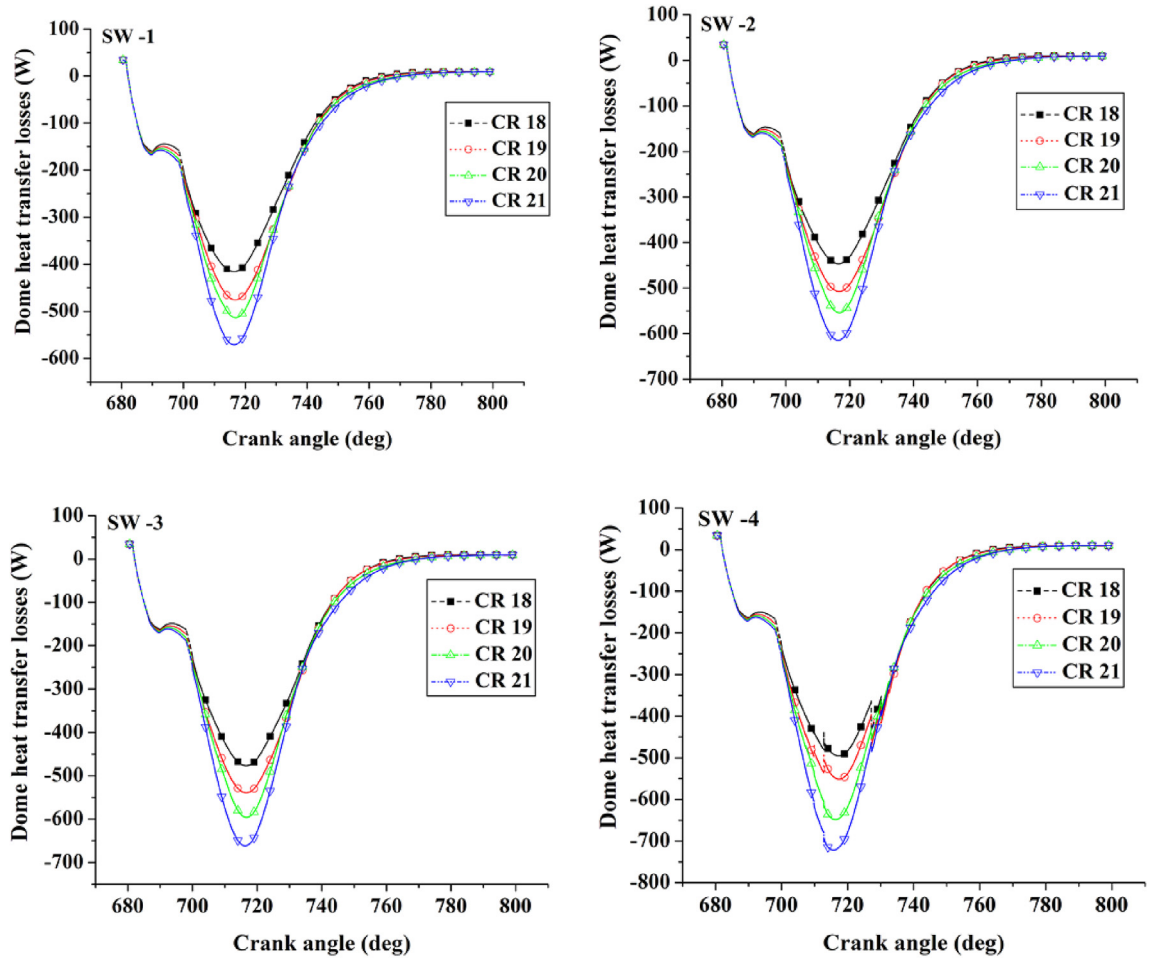

Fig. 14. Heat transfer to the domes Vs Crank angle at different compression ratios and swirl ratios.

Table 11
Heat Transfer to the dome (W) at various compression ratios and swirl ratios.

	SW1	SW2	SW3	SW4	Percentage increase between SW1–SW4
CR 18	−415.888	−446.574	−477.041	−495.458	**19.13**
CR 19	−475.69	−507.495	−539.222	−551.386	**15.91**
CR 20	−513.628	−554.096	−596.019	−648.456	**26.25**
CR 21	−570.898	−614.603	−661.657	−721.727	**26.41**
Percentage Increase between CR 18-CR 21	**37.27**	**37.62**	**38.70**	**45.66**	

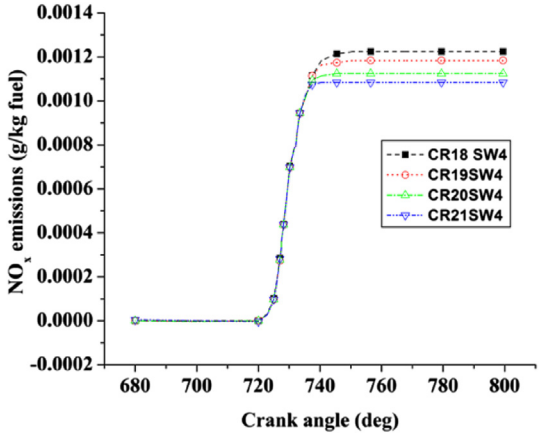

Fig. 15. NO_x emissions Vs Crank angle.

increase in EGR the NOx emissions were observed to be decreasing irrespective of swirl ratio. Maximum reduction in Nox emissions was observed with 30% EGR and swirl ratio 4.

It was observed that maximum increased heat transfer rates of 0.88% to the wall with swirl ratio 1, 45.66% to the dome and 39.99% to the piston with swirl ratio 4; when the compression ratios are increased from 18 to 21. A maximum increase in heat transfer rates of 15.82% to the wall, 26.41% to the dome and 27.46% to the piston with compression ratio 2; when the swirl ratio is increased from 1 to 4.

The study revealed that apart from adopting higher compression ratios and boost pressures adoption of high swirl ratios is observed to be contributing to a large extent in enhancing the rates of heat transfer which would lead to significant reduction in in−cylinder temperatures suitable for low NOx emission formation in HCCI mode.

Acknowledgments

The authors thank Dr. Raja Banerjee, Associate Professor, IIT Hyderabad for allowing to use computational facility, Mr. B. Siva Nageswara Rao from CD-adapco, Bengaluru and Mr. P. Madhu computer Lab supervisor IIT Hyderabad for their support during the simulation work.

References

[1] Epping, K., Aceves, S. M., Bechtold, R. L., and Dec, J. E, The Potential of HCCI Combustion for High Efficiency and Low Emissions, SAE Paper No. 2002-01-1923.
[2] Karthikeya Sharma T, Amba Prasad Rao G, Madhumurthy K. Combustion analysis of ethanol in HCCI engine. Trends Mech Eng 2012;3(1).
[3] Manimaran Renganathan, Thundil Karuppa Raj Rajagopal. Computational studies of swirl ratio and injection timing on atomization in a direct injection diesel engine. Front Heat Mass Trans (FHMT) 2014;5(1).
[4] Venkateswaran S Pasupathy, Nagarajan G. Effects of the re-entrant bowl geometry on a DI turbocharged diesel engine performance and emissions—a CFD approach. J Eng Gas Turb Power 2010;132(12):122803.
[5] Maroteaux F, Noel L, Ahmed A. Numerical investigations on methods to control the rate of heat release of HCCI combustion using reduced mechanism of n-heptane with a multidimensional CFD code. Comb Theory Model 2007;11(4):501–25.
[6] Karthikeya Sharma, T., Amba Prasad Rao, G., madhumurthy, K., Effect of swirl of performance and emissions of CI engine in HCCI mode. doi 10.1007/s40430-014-0247-7.
[7] Duclos JM, Zolver M, Baritaud T. 3D modeling of combustion for DI-SI engines. Oil Gas Sci Tech Rev IFP 1999;54(2):259–64.
[8] Colin O, Benkenida A. The 3-zone extended coherent flame model (ECFM3Z) for computing premixed/diffusion combustion. Oil Gas Sci Tech Rev IFP 2004;59(6):593–609.
[9] Ravet F, Abouri D, Zellat M, Duranti S. Advances in combustion modeling in STAR-CD: validation of ECFM CLE-H model to engine analysis. In: 18th Int Multdl Eng Users' Meet SAE Congress – Detroit; 2008, April, 13.
[10] Subramanian, G., Vervish, L. and Ravet, F., New Developments in Turbulent Combustion Modeling for Engine Design: ECFM-CLEH Combustion Sub Model, SAE Int – 2007-01-0154.
[11] Moureau V, Lartigue G, Sommerer Y, Angelberger C, Colin O, Poinsot T. Numerical methods for unsteady compressible multi-component reacting flows on fixed and moving grids. Int J Comput Phys 2005;202(2):710–36.
[12] Zellat, Marc, Stefano Duranti, YongJun Liang, Cedomir Kralj, Gerald Schmidt, Jean-Marc Duclos. Towards a universal combustion model in STAR-CD for IC engines: from GDI to HCCI and application to DI Diesel combustion optimization. In: Proceedings of 14th International Multidimensional Engine User's Meeting, SAE Cong; 2005.
[13] Y.Bakhshan, Multi-dimensional simulation of n-heptane combustion under hcci engine condition using detailed chemical kinetics. J Engine Res, 22.
[14] Ganesh D, Nagarajan G. Homogeneous charge compression ignition (HCCI) combustion of diesel fuel with external mixture formation. Energy 2010;35(1):148–57.
[15] García Miguel Torres, Aguilar Francisco José Jiménez-Espadafor, Lencero Tomás Sánchez, Villanueva José Antonio Becerra. A new heat release rate (HRR) law for homogeneous charge compression ignition (HCCI) combustion mode. Appl Therm Eng 2009;29(17):3654–62.
[16] Soyhan HS, Yasar H, Walmsley H, Head B, Kalghatgi GT, Sorusbay C. Evaluation of heat transfer correlations for HCCI engine modeling. Appl Therm Eng 2009;29(2):541–9.
[17] Christensen Magnus, Johansson Bengt, Amnéus Per, Mauss Fabian. Supercharged homogeneous charge compression ignition. SAE Technical paper. 1998. No. 980787.
[18] Hyvönen Jari, Haraldsson Göran, Johansson Bengt. Supercharging HCCI to extend the operating range in a multi-cylinder VCR-HCCI engine. 2003. No. 2003-01-3214. SAE Technical Paper.
[19] Genzale CL, Kong SC, Reitz RD. Modeling the effects of variable intake valve timing on diesel HCCI combustion at varying load, speed, and boost pressures. J Eng Gas Turb. Power 2008;130(5):052806.
[20] Chmela, Franz G., and Gerhard C. Orthaber, "Rate of heat release prediction for direct injection diesel engines based on purely mixing controlled combustion", No. 1999-01-018, SAE Technical Paper-1999.
[21] Choi Seungmok, Park Wonah, Lee Sangyul, Min Kyoungdoug, Choi Hoimyung. Methods for in-cylinder EGR stratification and its effects on combustion and emission characteristics in a diesel engine. Energy 2011;36(12):6948–59.
[22] Neshat Elaheh, Saray Rahim Khoshbakhti. Effect of different heat transfer models on HCCI engine simulation. Energy Convers Manag 2014;88:1–14.
[23] Johansson Thomas, Johansson Bengt, Tunestål Per, Aulin Hans. Turbocharging to extend HCCI operating range in a multi cylinder engine-benefits and limitations. In: World automotive Congress, FISITA; 2010. p. 1–14.
[24] Lu Xingcai, Qian Yong, Yang Zheng, Han Dong, Ji Jibin, Zhou Xiaoxin, et al. Experimental study on compound HCCI (homogenous charge compression ignition) combustion fueled with gasoline and diesel blends. Energy 2014;64:707–18.